

Load-Dependent Muscle Efficiency, as Measured in Whole Muscles, Muscle Fibers, Myofibrils and Myosin Heads

Haruo Sugi*

*Department of Physiology, Teikyo University Medical School, Tokyo, Japan.

Received April 02, 2018; Accepted April 22, 2018; Published June 26, 2019

ABSTRACT

This article deals with the history of research work to obtain the efficiency, with which a muscle converts chemical energy into mechanical work. In 1923, Fenn found that energy output (heat H plus work W) in contracting muscle changed depending on the load, indicating that biological systems can regulate their energy output depending on external conditions. The ratio $W/(H+W)$ was called mechanical efficiency, and its load-dependence was found to be bell-shaped, being maximum (0.36) at an intermediate load. Since the heat production in contracting muscle contains thermoelastic heat and heat for Ca^{2+} cycling, the word, mechanical efficiency, was proved to be inadequate. After ATP was proved to be the immediate energy source for contraction, experiments are performed with single permeabilized muscle fibers, where contraction can be produced by externally applied Ca^{2+} , while ATP hydrolysis can be measured using NADH fluorescence or Pi-sensitive fluorescent protein. The dependence of the efficiency, with which energy of ATP hydrolysis is converted into mechanical work, on the load or the isovelocity shortening was bell-shaped, being maximum (0.25—>0.5) at an intermediate load or velocity. Similar results were obtained using single myofibrils using a fluorescent ATP analog, Cy3-EDA ATP. We have estimated the efficiency of individual myosin heads by performing experiments, in which almost all myosin heads within a permeabilized muscle fiber are in the state of M-ADP-Pi, so that on laser flash photolysis of caged Ca^{2+} , individual myosin heads perform power stroke only once, thus avoiding asynchronous performance of myosin heads. We estimated the amount of ATP utilized for contraction by measuring the redevelopment of tension after quick releases applied to isometrically contracting fibers, or after clamping length of shortening fibers. Assuming an appropriate value of energy released from one ATP molecule, the efficiency of individual myosin head was calculated to be > 0.7 . As this estimation is conservative, it is suggested that the actual efficiency is close to unity.

Keywords: Muscle efficiency, Mechanical efficiency, Muscle contraction, Muscle fiber, Myofibril, Myosin head, Muscle heat production, Muscle work production

HISTORICAL BACKGROUND: THE FENN EFFECT

In 1923, W.O. Fenn attached a frog muscle in an inertial lever system (**Figure 1**, inset) and made it to contract with a single electrical stimulus [1]. The muscle first shortened actively by moving the inertial lever, and then went slack after by the continuing movement of the inertial lever, and was finally lengthened by a light weight w attached to an isotonic lever. With this device, Fenn succeeded in recording muscle heat production H and work done W during its active contractile activity, without complications arising from heat production during passive muscle lengthening. As shown in Figure 1, the amount of energy output ($H+W$) was found to be maximum at an intermediate inertial load. The finding of Fenn is called “the Fenn effect”, and regarded as the first indication of biological systems like muscle that they have

ability to regulate their energy output depending on experimental conditions.

Corresponding author: Haruo Sugi, Department of Physiology, Teikyo University Medical School, Tokyo, Japan, Tel: +81 484 78 4079; E-mail: sugi@kyf.biglobe.ne.jp

Citation: Sugi H. (2019) Load-dependent Muscle Efficiency, as Measured in Whole Muscles, Muscle Fibers, Myofibrils, and Myosin Heads. *Adv Nanomed Nanotechnol Res*, 1(1): 1-18.

Copyright: ©2019 Sugi H. This is an open-access article distributed under the terms of the Creative Commons Attribution License, which permits unrestricted use, distribution, and reproduction in any medium, provided the original author and source are credited.

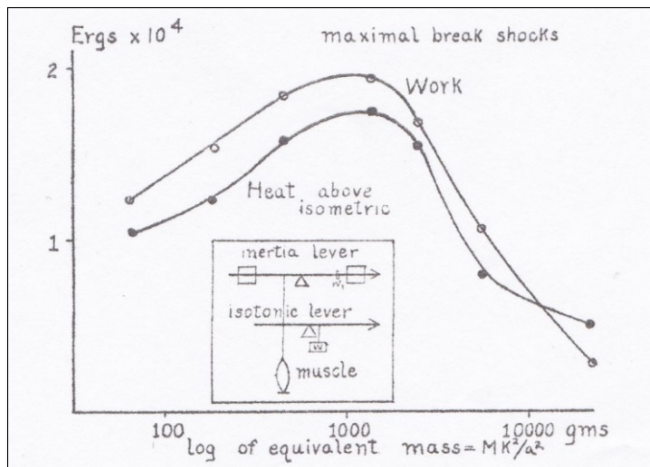


Figure 1. Dependence of work done by muscle (open circles) and heat liberated from shortening muscle above that from muscle kept isometric (filled circles) on the inertial load.

Inset shown the inertial lever system. The muscle first shortens by moving the inertial lever, and after its mechanical activity is over, is lengthened by a light weight w to its initial length [1]

The Fenn effect made Hill to throw away his viscoelastic model, which predicted that the amount of energy output ($H+W$) was constant for a given amount of muscle shortening and Hill and his coworkers started studying the dependence of energy output in muscles contraction, using an isotonic lever system, illustrated in **Figure 2**, with which muscles were stimulated to shorten under constant after loads, or held isometric to generate isometric force. **Figure 3** shows general features of tension and length changes in muscle during twitches under three different amounts of afterload and under the isometric condition [2]. It can be seen that, on stimulation, muscle first generates isometric tension to a value equal to the amount of afterload, and then muscle shortens with a constant velocity for a considerable fraction of time during muscle shortening, while the tension

(=amount of afterload) stays constant. As shown in **Figure 4**, the P versus V relation is a part of rectangular hyperbola, which can be expressed as $(P+a)(V+b) = b(P_0 - P)$, where a and b are constants (Hill equation). A most important feature of the after loaded shortening is that, when the isometric force generated muscle reaches the amount of afterload, muscle shortening takes place with a constant velocity, i.e., shortening without acceleration. This suggests that contracting muscle can somehow sense the amount of afterload during the isometric tension generation preceding shortening, to regulate its rate of energy output (=power). Reflecting the hyperbolic shape of P versus V relation, the rate of energy output (=power) is maximum at an intermediate load.

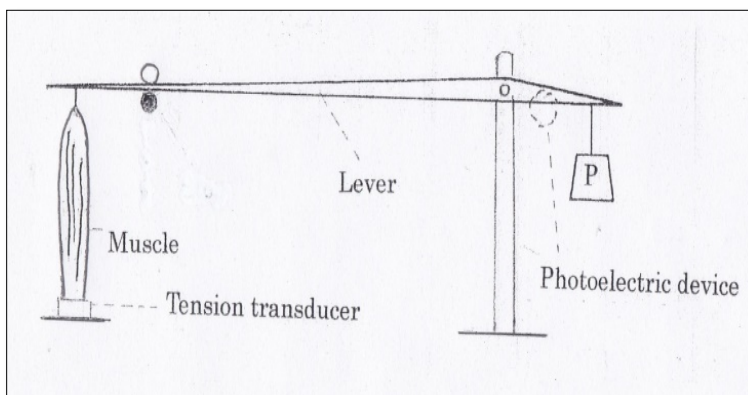


Figure 2. Experimental apparatus used for after loaded muscle contraction.

A muscle with one end fixed in position is connected to the tip of the long arm of a lever rotating around the axle. Various isotonic afterloads P are applied to the short arm the lever. Muscle lengthening by the load is prevented by an after load stop (open circle). Muscle shortening is recorded electronically by a photoelectric device at the short lever arm, while tension is measured by a tension transducer at the fixed end of muscle. To measure the maximum isometric tension, lever movement is prevented by another stop (filled circle)

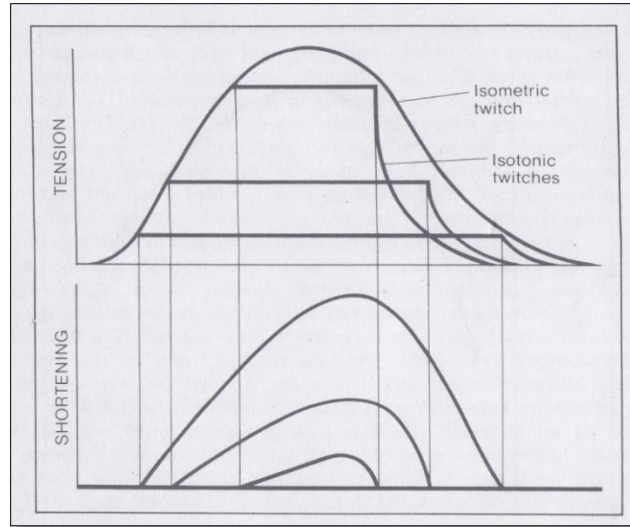


Figure 3. Tension (upper traces) and length (lower traces) of contracting muscle during a series of after loaded isotonic twitches.

Note that the muscle first contracts isometrically and as soon as the tension generated exceeds the amount of afterload, muscle starts shortening isotonicly under a constant afterload [2]

Figure 5 summarizes the results of experiments, in which both heat H produced, and work W done by contracting muscle during a short tetanus are measured simultaneously [3]. The energy output ($H+W$) versus load relation was bell-shaped as reported by Fenn and the mechanical efficiency ($W/H+W$) was also maximum at an intermediate load, being ~ 0.3 . The experiments with whole muscle contain a number of uncertainties listed below: (1) whole muscles consist of a number of muscle fibers with different characteristics, resulting in considerable non uniformities in both longitudinal and transverse directions; (2) non uniform contact of the thermopile to muscle makes the correlation

between H and W , and (3) the period of heat measurement extends arbitrarily for many seconds after completion of muscle contraction without any concrete basis. (4) Heat production results not only from muscle contraction, but also from other phenomena such as thermoelastic heat and reactions concerned with Ca^{2+} cycling. Consequently, although the maximum mechanical efficiency of contracting muscle was estimated to be ~ 0.3 , it was proved to be inappropriate to represent the actual muscle efficiency in producing mechanical work. In this article, we shall hereafter use the word, efficiency, instead of mechanical efficiency defined by Hill.

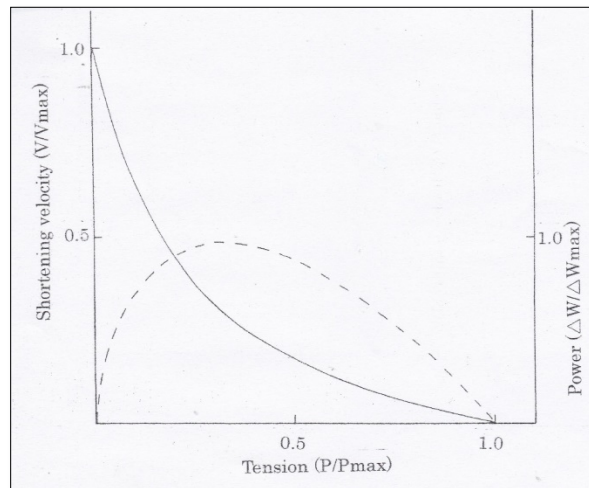


Figure 4. Dependence of the shortening velocity V (solid line) and the power, i.e., the rate of energy output $\Delta W (=V \times P$, broken line) on the amount of afterload P during a twitch in frog skeletal muscle.

Both V and P are expressed relative to their maximum values V_{max} and ΔW_{max} , respectively. Note hyperbolic $P-V$ relation and bell-shaped $P-\Delta W$ relation [2]

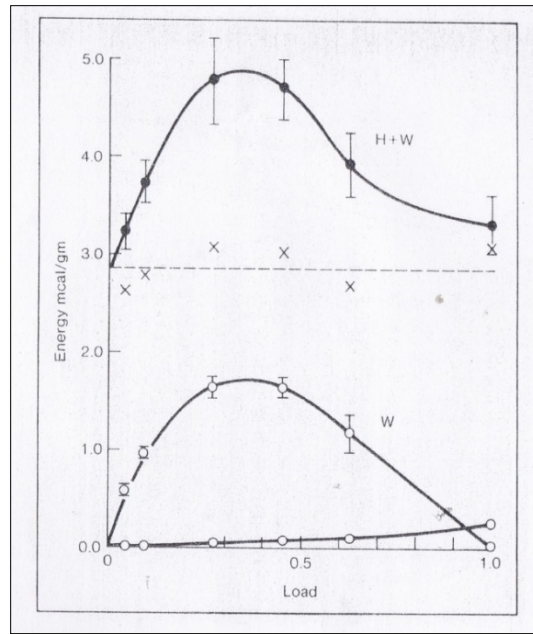


Figure 5. Load dependence of total energy output (heat H plus work W, filled circles, and work (W, open circles) during a short tetanus.

Work consists of external work (upper curve) and internal work (lower curve) done by stretching internal elastic component. Crosses indicate heat minus work [4]

STUDIES ON CHEMICAL CHANGES IN CONTRACTING MUSCLE

Progress in biochemical studies on muscle has made it gradually clear that ATP is the only immediate source of energy for muscle contraction. In relaxed muscle, the ATP concentration is kept low, and is therefore insufficient to support muscle activity for a long period. During sustained muscle activity, ATP is continuously resynthesized by the Lohman reaction from ADP and phosphocreatine (Cr-P), as $\text{Cr-P} + \text{ADP} \rightarrow \text{Cr} + \text{ATP}$, so that, during contraction, ATP concentration does not change appreciably, while phosphocreatine concentration decreases as long as contraction goes on. This was ascertained by a number of investigators by quickly freezing muscle after

Completion of its mechanical activity and measuring the phosphocreatine concentration in muscle [3-6]. The results are summarized in **Figure 6**. Irrespective of the types of contraction, the amount of PCr breakdown (ΔPCr) is proportional to that of energy output (heat+work). The results can be taken only qualitative, because muscle weight is not accurate because of variable water content in muscles. In 1962, Cain and Davies [7] found that fluorodinitrobenzene (FDNB) was an inhibitor of the Lohmann reaction. Using FDNB, it was also shown by many authors

that a good correlation existed between the amount of work done by contracting muscle and the amount of ATP hydrolyzed [7-10] (**Figure 7**). **Figure 8** shows the estimation of muscle efficiency to convert energy derived from ATP hydrolyzed into mechanical work. The efficiency is maximum (>0.5) at the intermediate shortening velocity ($\sim 0.3 V_{\text{max}}$), being much higher than the values determined by measuring heat and work. The estimation of efficiency using whole muscles and chemical analysis has a number of problems and uncertainties, so that the values obtained are far from being convincing. A most serious short coming in the use of whole muscles is non-uniformity of sarcomere length, since sarcomere length determines the number of myosin heads, producing tension and shortening in muscle. Without controlling sarcomere length in muscle preparation, it is impossible to estimate muscle efficiency. For this reason, some investigators cast doubt even on the Fenn effect, since it might result from an increase in the number of myosin heads caused by muscle shortening. As will be described later in this article, the Fenn effect was confirmed in experiments with single muscle fibers and single myofibrils, in which sarcomere length was controlled accurately, suggesting that the Fenn effect might originate from the property of individual myosin heads. This point will become clear later in this article.

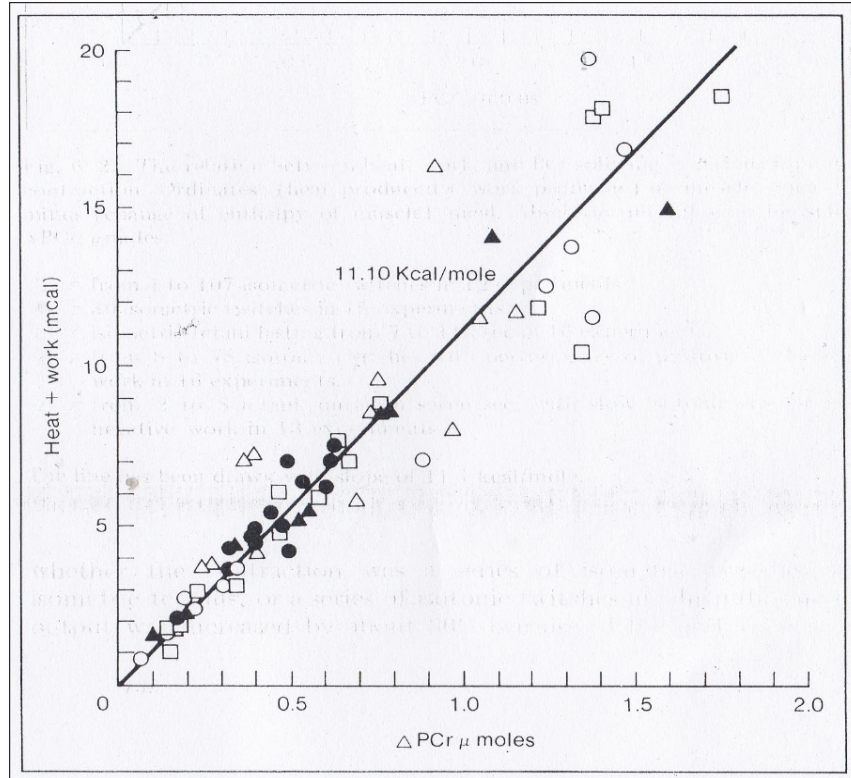


Figure 6. Relation between energy output (heat + work) and phosphocreatine splitting (ΔPCr) in various types of muscle mechanical activity. The straight line is drawn with slope of 11.1 kcal/mol. Seventy-two different muscles were made to contract isometrically, isotonicly or being stretched during twitches and tetani. Different symbols indicate different types of experiments [3]

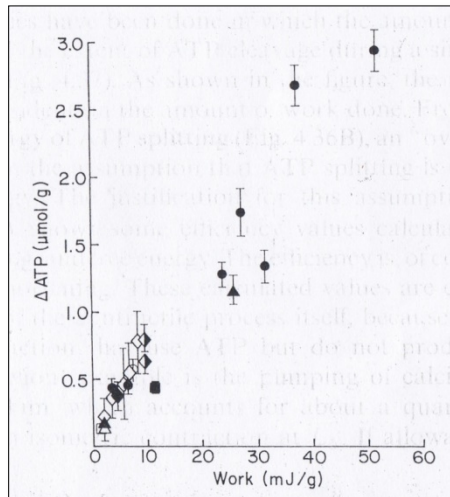


Figure 7. Relation between the amount of work done by contracting muscle and the amount of ATP hydrolyzed. Different symbols indicate different type of experiments [11]

Meanwhile, in the hyperbolic velocity versus relation shown in **Figure 4**, $V=0.3 V_{max}$ at $P(\text{load})=0.3 P_{max}$. Consequently, the result in **Figure 8** can also be stated that the efficiency is maximum at a load of $\sim 0.3 P_o$, where the rate of energy output is maximum. As can be seen in **Figure 3**, a muscle

first contracts isometrically and when the tension generated by muscle reaches the value equal to the load it starts shortening with a constant velocity. It seems therefore natural to consider that, during the initial isometric tension generation, the muscle senses the amount of load imposed

on it, and determines the rate of energy output during the subsequent period of isotonic shortening. In this sense, it was a misleading that the authors expressed the efficiency as a function of shortening velocity, but not amount of load. In

our personal feeling, it is strange that discussions are still made from time to time as to whether shortening velocity or load determines the rate of energy output.

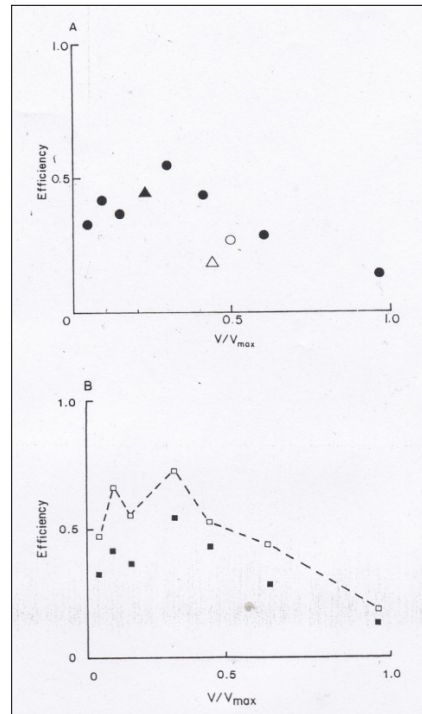


Figure 8. Dependence of the muscle efficiency (work W/free energy) on the shortening velocity.

Note that the efficiency is maximum at a velocity of $\sim 0.3 V_{max}$ [11]

In this article, we will present evidence that the energy output is determined by the load even at the level of individual myosin heads.

SIMULTANEOUS RECORDING OF ATP HYDROLYSIS AND MECHANICAL RESPONSE IN PERMEABILIZED SINGLE MUSCLE FIBERS

A skeletal muscle is composed of muscle fibers (diameter, 50-100 μm), which in turn contains myofibrils (diameter, $\sim 1 \mu\text{m}$). Both muscle fibers and myofibrils exhibit cross-striation. As illustrated in **Figure 9**, the structural unit of cross-striation is the sarcomere, in which actin filaments, consisting of two helical strands of globular actin monomers, extends from Z-line in between myosin filaments located central in the sarcomere. Myosin filaments are composed of myosin molecules, each consisting of two heads and a long rod. The rods aggregate to form myosin filament backbone,

while myosin heads extend laterally facing actin filaments. It is well established that muscle contraction results from attachment-detachment cycle between myosin heads and actin filaments, coupled with ATP hydrolysis. The number of myosin heads, which can interact with actin filaments to produce tension and shortening in muscle, in each sarcomere depends on the extent of overlap between actin and myosin filaments, i.e., the length of sarcomere [11,12]. In experiments with whole muscles, it was impossible to control sarcomere length in the component muscle fibers. In experiments with single muscle fibers and single myofibrils, sarcomere length can be measured and controlled by light diffraction with He-Ne laser light. Normally, the initial sarcomere length is adjusted to 2.4 μm , so that the number of myosin heads interacting with actin filaments is kept fairly constant.

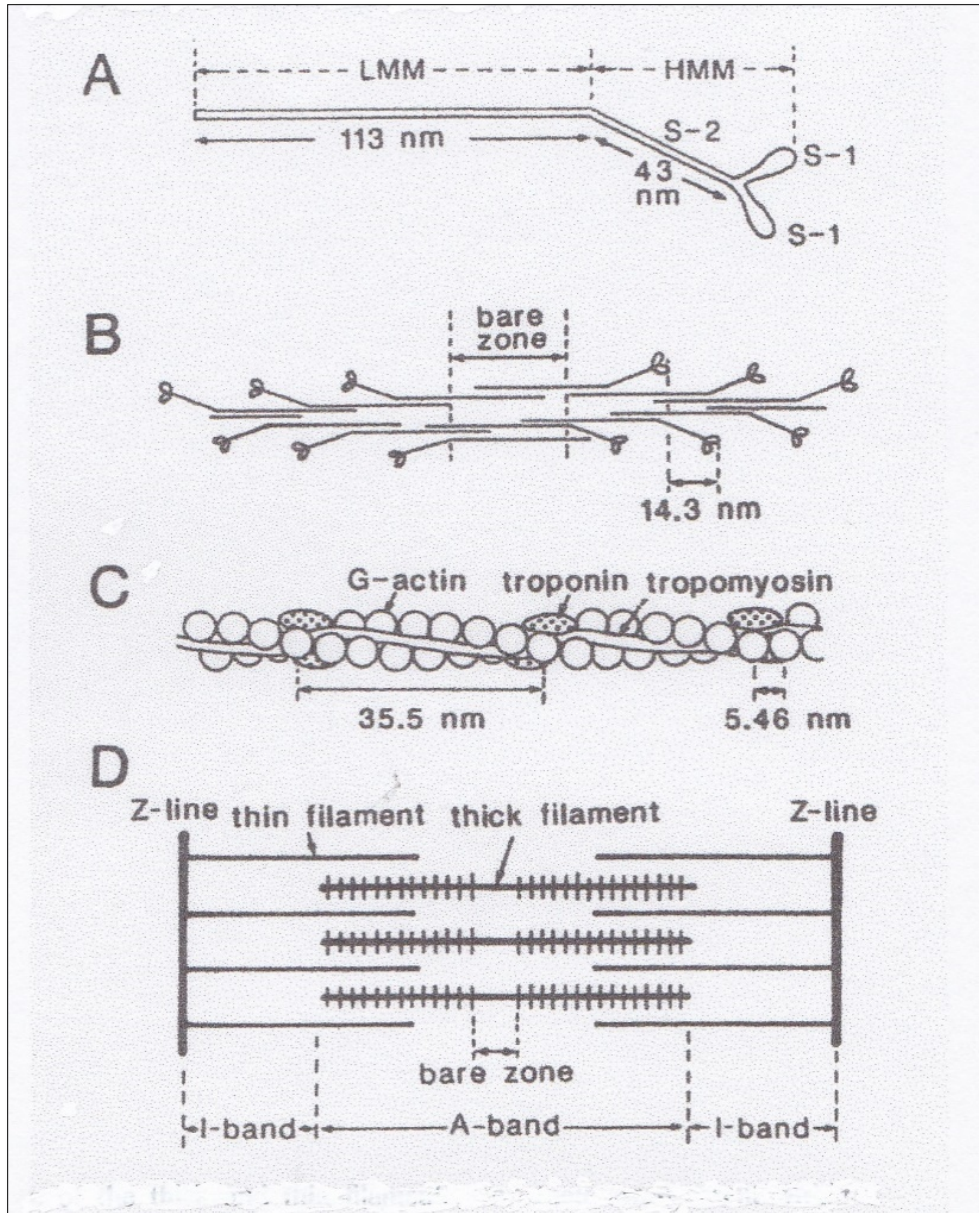


Figure 9. Structure of myosin molecule, myosin and actin filaments and their arrangement in a sarcomere. (A) Myosin molecule consisting of two heads and a long rod. (B) Myosin filament, in which myosin rods form filament backbone while myosin heads extend laterally. (C) Actin filament consisting of two helical strands of actin monomer. (D) Arrangement of actin and myosin filaments in a sarcomere. Short vertical bars extending from myosin filaments represent myosin heads [12].

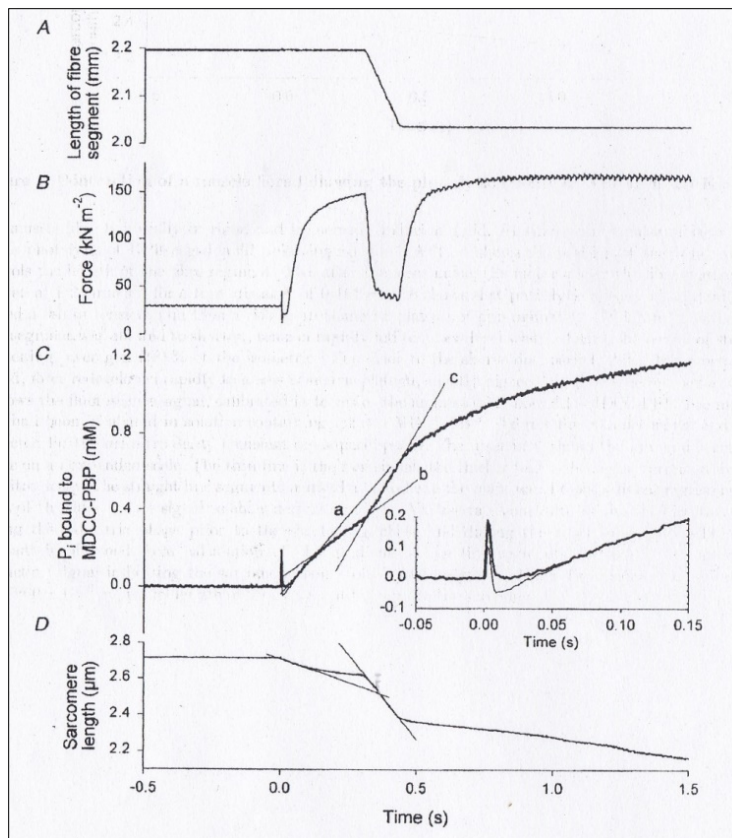


Figure 10. Laser flash-induced Contraction of a single permeabilized muscle fiber. (A) Constant velocity fiber shortening with a servo-motor. (B) Tension (=force) changes in the fiber caused by the fiber shortening. (C) Release of P_i resulting from ATP hydrolysis, recorded by fluorescence changes of P_i -sensitive protein, MDCC-PBP. Inset shows the initial fluorescence change on an expanded time base. (D) Change in sarcomere length, recorded by He-Ne laser light [16].

In addition to the advantages explained above, problems arising from the use of whole muscles with respect to measurement of chemical changes in them can also be removed by using single permeabilized muscle fibers, in which surface membrane is removed by various ways, so that externally applied chemical compounds such as ATP can enter into the interior of the fiber. Permeabilized muscle fibers can be maximally activated to contract by putting them from relaxing solution ($pCa > 9$) to contacting solution ($pCa, 4$) [13]. The rate of ATP utilization in permeabilized muscle fibers is most widely recorded by using phosphoenol pyruvate (PEP) and nictinamide adenine dinucleotide (NADH) as follows: (1) ATP hydrolysis into ADP and inorganic phosphate (P_i), $ATP \rightarrow ADP + P_i$; (2) ADP reacts with PEP to yield pyruvate and ATP, $ADP + PEP \rightarrow ATP + pyruvate$; (3) pyruvate reacts with NADH to yield NAD^+ and lactate, $pyruvate + NADH \rightarrow NAD^+ + lactate$. Thus, ADP production resulting from ATP hydrolysis is recorded photometrically as decrease in NADH absorbance at 340 nm [14]. To avoid movement artefact, recording of NADH absorbance changes are made outside the fiber. Using the above method, the maximum efficiency of 0.25 and 0.28 in

permeabilized fibers has been estimated to be 0.25 or 0.28 [15].

He et al. [16] on the other hand, used a fluorescent protein, MDCC-PBP, which binds with P_i and changes its fluorescence, to continuously recording the amount of ATP hydrolyzed during muscle fiber contraction by recording the MDCC-PBP fluorescence, serving as a measure of P_i liberated by ATP hydrolysis. To activate permeabilized fibers uniformly and rapidly, they used the method of laser flash photolysis of caged ATP, a compound that releases ATP on photolysis with intense laser light flash. They also continuously recorded sarcomere length of the fiber by recording light diffraction with He-Ne laser light. It can be seen in **Figure 10** that, during application of constant-velocity shortening (record A), the tension in muscle falls to a low steady level, and after completion of shortening tension redevelops to a steady level (record B). The rate of P_i liberation, i.e., the rate of ATP hydrolysis, is initially rapid and then approaches to a constant rate, as indicated by lines a and b showing the slope of the record and again increases to a high rate indicated by line c on application of shortening to the fiber (record c). This shows clearly that the

Fenn effect can still be observed in experiments, in which all ambiguities and uncertainties inherent to whole muscle experiments are removed. Assuming the free energy of ATP hydrolysis to be 50 kJ/mol, the maximum efficiency of

muscle fiber contraction was estimated to be 0.36 at an applied shortening velocity of $\sim 0.27 V_{\max}$, corresponding to tension at 0.51 Po (**Figure 11**).

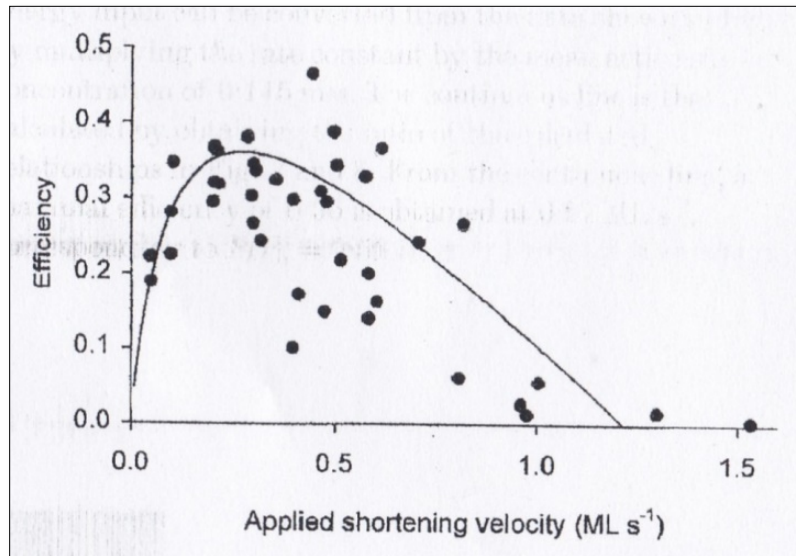


Figure 11. Relation between the efficiency of muscle fiber contraction and the applied constant velocity shortening. Note that the efficiency is maximum (~ 0.36) at shortening velocity $\sim 0.27/V_{\max}$, corresponding to tension $\sim 0.51 Po$ [16]

THE FENN EFFECT IS OBSERVED IN BOTH MUSCLE MYOFIBRILS AND *IN VITRO* MOTILITY ASSAY SYSTEMS

To further study the relation between the rate of ATP hydrolysis and mechanical response at the level of myofibrils constituting muscle fibers, we performed experiments on single myofibrils isolated from rabbit skeletal muscle fibers [17]. At the start of experiments, we expected that, at the level of single myofibrils, we might obtain results somewhat different from the Fenn effect, because it was obtained in a crude experimental condition compared to the current advanced experimental methods. We used a fluorescent nucleotide analog, Cy3-EDA-ATP to record ATP hydrolysis. It was necessary to use a confocal

microscope to reduce background noise for accurate recording of fluorescent changes in myofibrils. As shown in **Figure 12**, fluorescence is localized in the A-band in each sarcomere, where myosin filaments and therefore myosin heads are located. On simultaneous application of Ca^{2+} and ATP released from caged ATP, Cy3-ATP in the myofibril is hydrolysed by myosin heads to be replaced by non-fluorescent ATP. By applying isovelocity shortening to activated myofibrils with a piezo-electric device, we obtained the dependence of the rate of displacement of fluorescent ATP on the velocity of shortening, as shown in **Figure 13**. As has been the case in whole muscles and muscle fibers, the relation was bell-shaped; the maximum rate of ATP hydrolysis is maximum at a moderate shortening velocity.

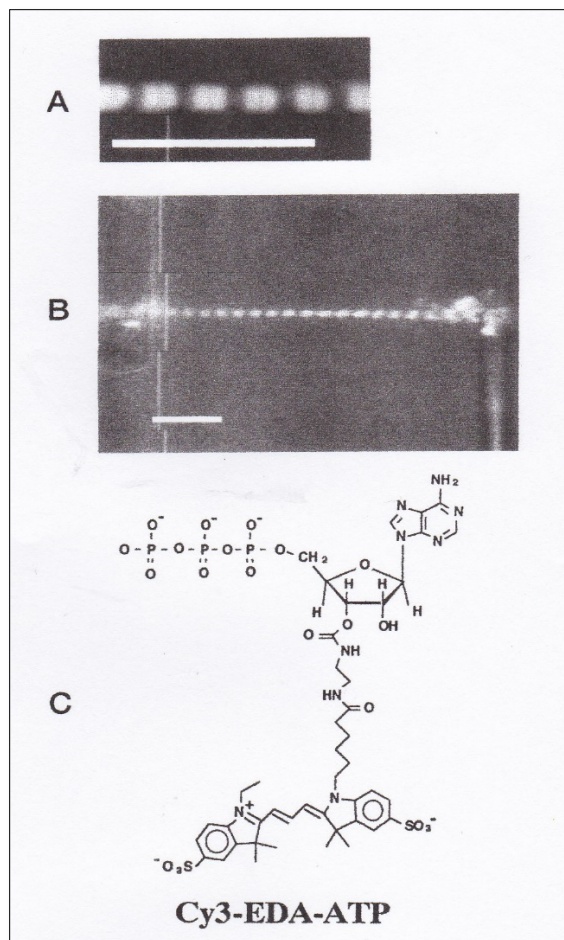


Figure 12. Use of fluorescent Cy3-EDA ATP to record ATP hydrolysis in isolate single myofibrils. (A) Enlarged view of myofibril showing Cy3-EDA ATP fluorescence localized in the A-band. (B) A single myofibril held between two glass needles, one fixed in position while the other connected to a piezo electric actuator. (C) Structure of Cy3-EDA ATP [17].

We also made experiments using an in vitro assay system, in which both tension and displacement caused by ATP-induced sliding of a myosin-coated glass micro needle (M) along well organized actin filament arrays (actin cables) in a giant algal cell (P) (**Figure 14A**) [18]. The myosin heads on the needle initially formed rigor linkages with actin cables, and on iontophoretic application of a constant amount of ATP released from the ATP containing electrode (A), started sliding along actin cables by bending the needle and eventually stopped moving after exhaustion of applied ATP. To remove ATP remaining in experimental solution, Hexokinase and D-glucose were added as ATP scavenger. By repeated applications of constant amount of ATP, myosin heads on the needle made work under various initial baseline tensions, at which the needle started moving (**Figure 14B**). The amount of work W done by myosin heads on the needle during the ATP-induced needle movement from position X_1

and position X_2 on actin cables is, $W = K [(X_2)^2 - (X_1)^2] / 2$, where K is elastic coefficient of the needle. As can be seen in **Figure 14C**, The W versus initial baseline tension is bell-shaped, the amount of W being maximum at $\sim 0.5 P_0$, i.e., the maximum isometric tension generated by myosin heads. Judging from the amount of P_0 , the number of myosin heads producing the needle movement appeared to be ~ 10 , indicating that the bell-shaped load dependence of work can be observed in a small number of myosin heads. The results suggest strongly that the Fenn effect originates from the fundamental property of individual myosin heads in myosin filament to regulate their energy output, but not from the property of numerous myosin heads within a muscle fiber to regulate the proportion of myosin heads working actively. This idea is supported by the experiments to be described in the next chapter.

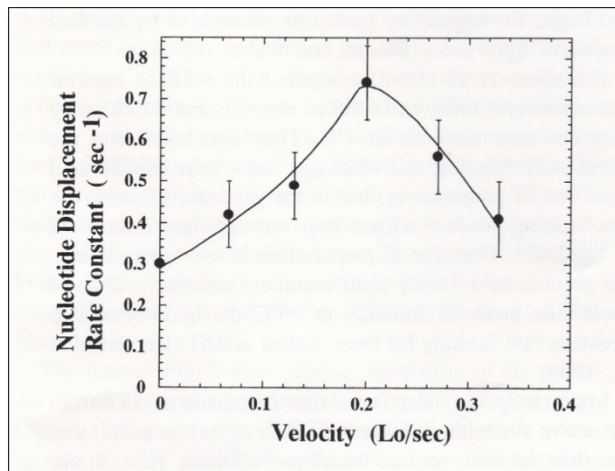


Figure 13. Bell-shaped relation between the rate of Cy3-EDA ATP displacement, i.e. the rate of ATP hydrolysis and the velocity of myofibril shortening [17].

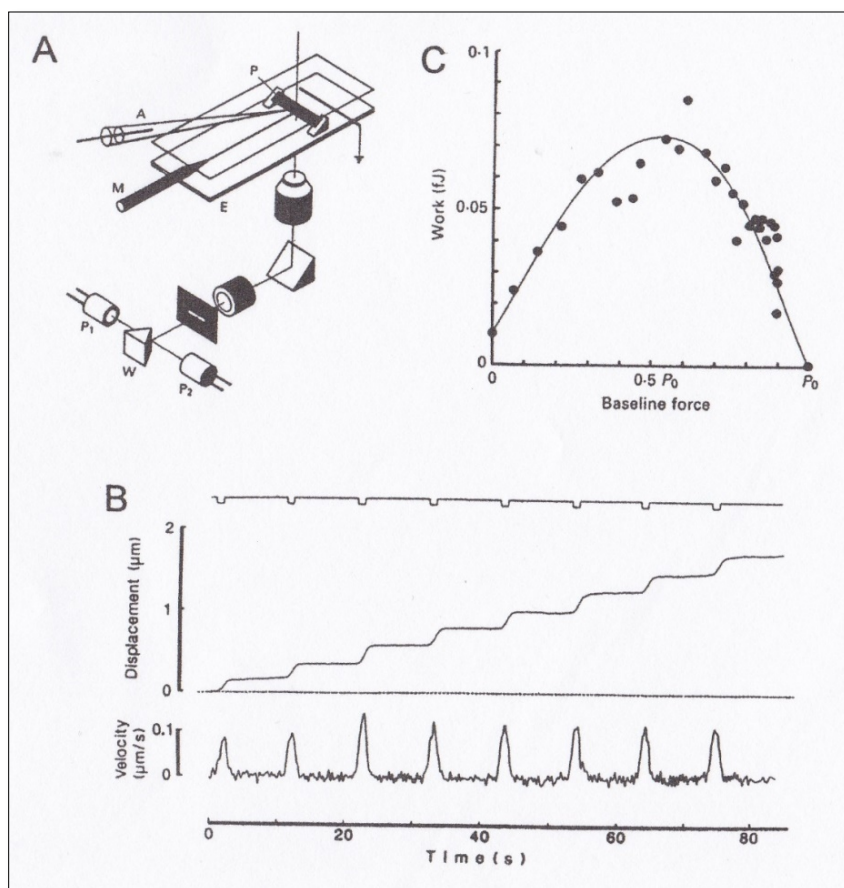


Figure 14. *In vitro* assay system to obtain relation between the initial baseline tension and the amount of work W done by myosin heads on a glass needle. (A) Diagram of experimental setup. Myosin coated glass microneedle M is made to slide along actin cables of a strip of giant algal cell P by applying a constant amount of ATP from the ATP-containing electrode A . The resulting microneedle movement is recorded with a wedge-shaped mirror W and a pair of photodiodes P_1 and P_2 . (B) Simultaneous recordings of constant current pulses to the ATP-containing electrode, to apply constant amount of ATP to myosin heads (upper trace), ATP-induced movement of the myosin-coated needle along actin cables (middle trace) and the velocity of needle movement (bottom trace) [18].

MEASUREMENT OF EFFICIENCY OF INDIVIDUAL MYOSIN HEADS DURING ISOTONIC SHORTENING IN SINGLE PERMEABILIZED MUSCLE FIBERS

In contracting muscle fibers, myosin heads repeat power strokes asynchronously. In other words, when a proportion of myosin heads within the fiber start performing power stroke, other myosin heads, which finished power stroke, may form rigor linkages with actin filaments to provide internal resistance against muscle contraction. This situation is well described by the contraction model of Huxley [19] as distribution of myosin heads producing positive and negative forces along the force axis during isotonic shortening. The actual efficiency of individual myosin heads in contributing muscle contraction is therefore masked by the asynchronous nature of myosin head performance. At the end of this article, we will describe our experiments with single permeabilized rabbit skeletal muscle fibers, in which the amount of ATP hydrolysed was estimated physiologically by recording the tension redevelopment following a quick release. For this purpose, we designed the following procedures based on the Lymn-Taylor scheme of ATPase reaction steps of actomyosin in solution. According to this scheme, in resting permeabilized muscle fiber, myosin heads (M) are in the state of M-ADP-Pi and when the fiber is activated by contracting solution. They attach to actin filaments (A) to form A-M-ADP-Pi to perform power stroke, producing tension and shortening, associated with reaction, $A-M-ADP-Pi \rightarrow A-M + ADP + Pi$. Then, if the ATP concentration within the fiber is adjusted to be almost equal to the number of myosin heads, almost all myosin heads are expected to be in the state of M-ADP-Pi, having long lifetimes >10 s.

We attempted to estimate the efficiency of individual myosin heads in the following way [20,21]: (1) Assuming

that the effective myosin head concentration within single muscle fiber is $\sim 150 \mu\text{M}$, we first put a single permeabilized fiber to experimental solution containing $220 \mu\text{M}$ ATP and 2.6 mM caged Ca (DM nitrophen); (2) after 40 min when the fiber showed a sign of development of rigor tension, namely, when the ATP concentration in the fiber decreased to a value close to that of myosin head concentration, the fiber was exposed in air and subjected to an intense laser flash to cause photolysis of caged Ca; and (3) the mechanical response of the flash-activated fiber was recorded under various afterloads imposed on the fiber with a servomotor system. In this way, almost all myosin heads within the fiber are expected to be in the state of M-ADP-Pi at the moment of flash activation, so that a large proportion of M-ADP-Pi myosin heads may start performing power stroke synchronously and then form rigor linkages with actin filaments. Consequently, the efficiency of individual myosin heads can be estimated by measuring the amount of work at the beginning of flash-induced contraction.

Figure 15 shows superimposed records of length (upper traces) and force (=tension) in a single permeabilized fiber during the laser flash-induced shortening under various amount of afterload. Because myosin heads perform power stroke only once and then form rigor linkages with actin filaments, the shortening velocity of flash-induced fiber did not exhibit constant velocity phase shown in **Figure 3**, but quickly decreased to zero. The time courses of power output by the flash-activated fiber under various afterloads are presented in **Figure 16**. It can be seen that the power output is maximum under a load of $0.35 P_o$. The abrupt rise of power output to a peak, which is observed for loads from 0.09 - $0.53 P_o$ seems to indicate that myosin heads perform power stroke almost synchronously in several milliseconds.

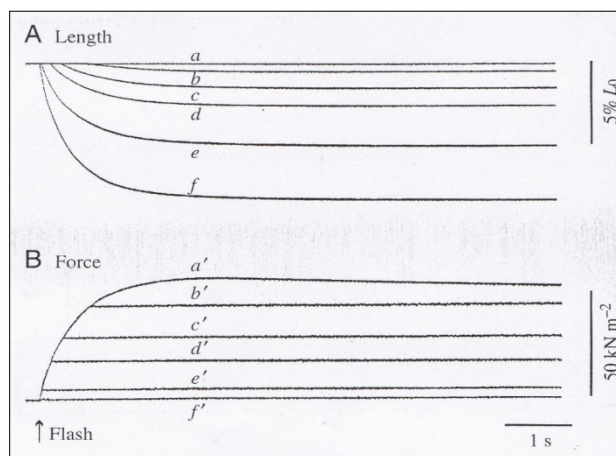


Figure 15. Superimposed length (A) and tension (B) changes in a permeabilized muscle fiber during laser flash-induced shortening under various afterloads. Records a to f in A correspond to records a' to f' in B. Records a, a' and f, f' are obtained during the isometric contraction and during practically unloaded shortening, respectively. Almost all myosin heads in the fiber were in the state of M-ADP-Pi at the moment of activation. The loads were P_o in a, a', $0.78P_o$ in b, b', $0.53 P_o$ in c, c', $0.35 P_o$ in d, d', $0.09 P_o$ in e, e' and practically zero in f, f' [20].

Figure 17 shows superimposed records of changes in fiber length (upper traces) and tension (lower traces), when a flash-activated fiber was allowed to shorten under various afterloads, and then subjected to quick changes in fiber length (quick releases) to drop the tension in the fiber to zero at 1s after flash activation. The amount of isometric tension redeveloped after the termination of isotonic shortening was regarded as a measure of amount of M-ADP-Pimyosin heads

which remained in the fiber after preceding isotonic shortening. Therefore, the amount of M-ADP-Pi myosin heads or the amount of ATP, utilized for the preceding isotonic shortening is estimated as $P_u = (P_o - P_r)$, where P_o is the maximum isometric force produced by flash-activated fiber and P_r is the amount of isometric force redeveloped after a quick release.

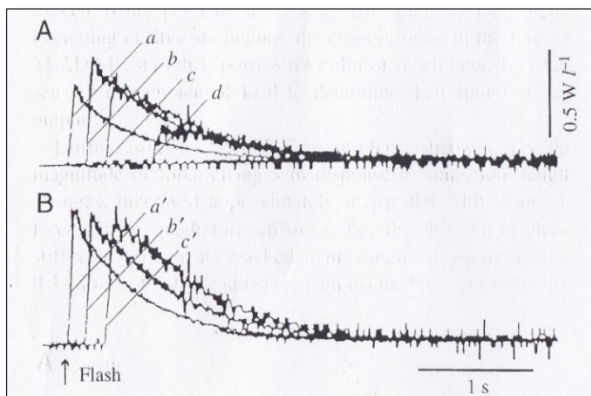


Figure 16. Superimposed records of power output in a permeabilized muscle fiber during flash-activated shortening under various afterloads (A) and the same records normalized with respect to peak values (B). The records were obtained from the experiment shown in **Figure 15**. The loads were 0.09 P_o in a, a', 0.35 P_o in b, b', 0.53 P_o in c, c' and 0.78 P_o in d, d' [21].

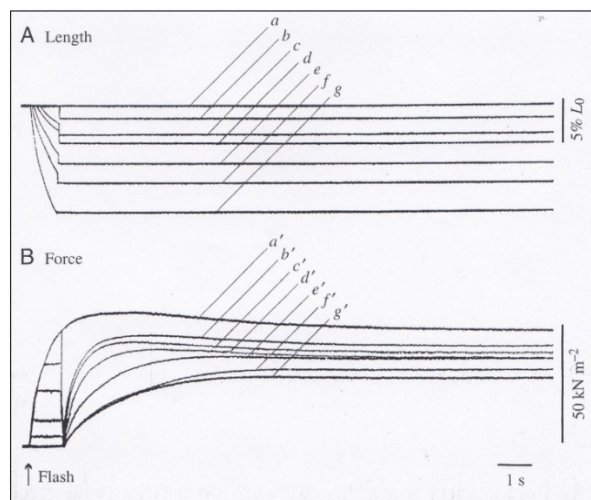


Figure 17. Superimposed records of length (A) and tension (B) changes in a permeabilized muscle fiber. The fiber was first made to shorten under various afterloads, and then subjected to quick releases to drop the tension to zero at 1 s after flash activation. After each release, the tension in the fiber redeveloped to various levels. Records a to g in A correspond to records a' to g' in B, respectively. The load was P_o in b, b', 0.63 P_o in c, c', 0.41 P_o in d, d', 0.20 P_o in e, e', 0.09 P_o in f, f' and zero in g, g', respectively. Records a, a' were obtained in the isometric condition [21].

Figure 18 is an example of experiments, in which the rate of ATP utilization is compared during generation of isometric tension (filled circles) and during shortening under a practically zero load (open circles). It is clear that the rate of ATP utilization is much larger during unloaded shortening than during isometric contraction. **Figure 19** shows the bell-shaped dependence of work (W) done by the flash-activated

fibers (open circles) and the amount of ATP (P_u) utilized for producing work W (P_u , filled circles) on the amount of afterload. The amount of work was maximum at the load of $\sim 0.4 P_o$, while the amount of ATP utilized is maximum during shortening under zero load and minimum during isometric contraction.

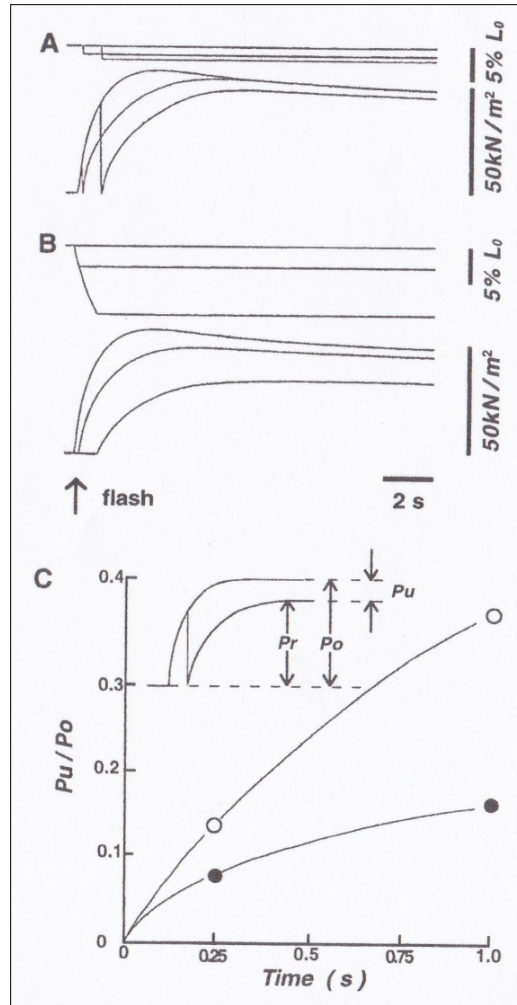


Figure 18. An example of experiments to obtain the amount of ATP utilized for contraction. (A) Superimposed records of fiber length (upper traces) and tension (lower traces) when a permeabilized fiber is first made to contract isometrically, and then subjected to a quick release to drop the tension to zero at 0.25 s or 1 s after flash activation. (B) Superimposed records of fiber length (upper traces) and tension (Lower traces) changes when the same fiber is first made to shorten under practically zero load, and then the fiber length is clamped at 0.25 s or 1 s after flash activation. (C) Changes in the value of P_u/P_o , serving as a measure of the amount of ATP utilized, with time after flash activation during isometric contraction (filled circles) and during shortening under zero load (open circles). P_u is obtained from difference between the maximum isometric tension P_o and the amount of tension redeveloped after a quick release P_r as illustrated in the inset [21].

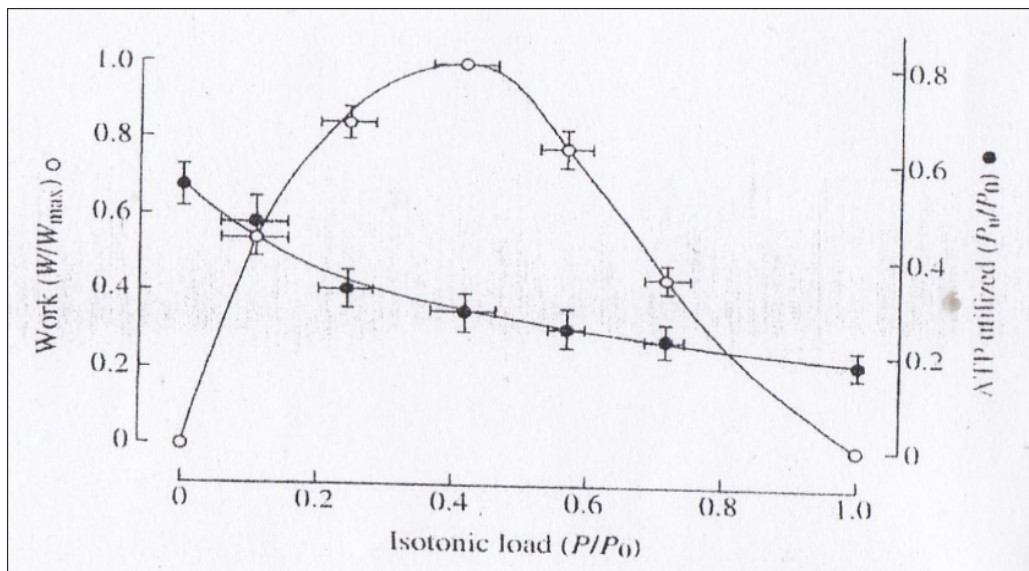


Figure 19. Dependence of the amount of work W (open circles) and the amount of ATP utilized (filled circles) on the amount of afterload in a permeabilized muscle fiber, in which almost all myosin heads are in the state of M-ADP-Pi at the moment of flash activation. Work and load are expressed relative to the maximum values as W/W_{max} and P/P_0 , respectively. The amount of ATP utilized was obtained as P_u/P_0 by the method shown in the inset of **Figure 18** [21].

The amount of ATP utilized for the whole mechanical response (P_u) is the sum of the ATP utilized for the initial isometric force development (P_i) and that for the subsequent isotonic shortening (P_s). The values of P_i as a function of isotonic load were obtained by applying quick releases to isometrically contracting fibers to drop the tension to zero at

various times after flash activation, and measuring the amount of force redevelopment following each release. **Figure 20** shows the results. Thus, the values of P_s were obtained by subtracting P_i for a given amount of tension equal to the load from the corresponding values of P_u for the whole mechanical response.

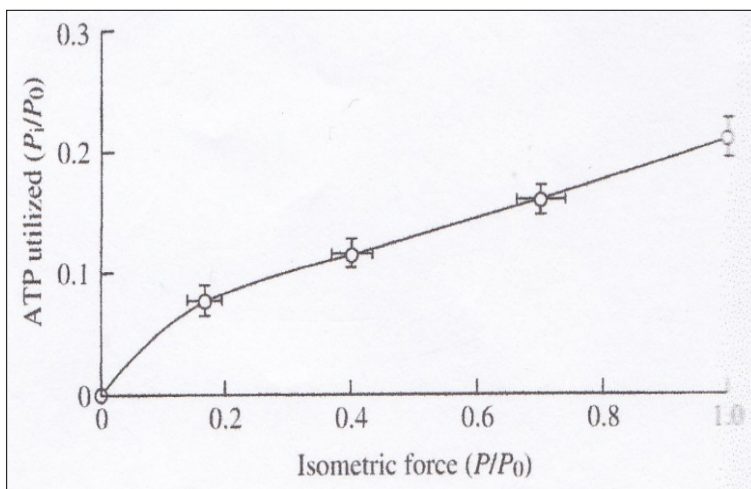


Figure 20. Relation between the amount of ATP utilized (P_i) and the isometric tension developed [21].

As can be seen in **Figure 21**, the values of P_s increased nearly linearly with the distance of fiber shortening irrespective of the amount of isotonic load. The relative value of efficiency of individual myosin heads (E), averaged over the period of work production, can thus be estimated as $E = W/(P_u - P_i) = W/P_s$, using the results in **Figures 20 and**

21. The dependence of E (expressed relative to the maximum value E_{max}) on the amount of isotonic load is shown schematically in **Figure 22**, together with values of W , P_u , P_i and P_s . The efficiency versus load relation was also bell-shaped, with a broad peak between 0.5 and 0.6 P_0 .

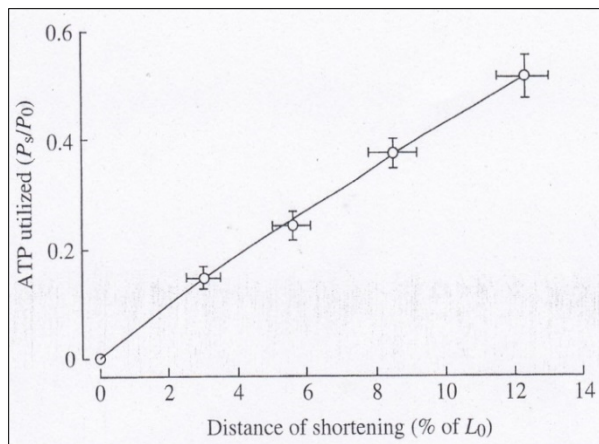


Figure 21. Dependence of the amount of ATP utilized (P_s) on the distance of isotonic shortening [21].

We tentatively calculated the absolute value of efficiency of individual myosin heads from the values of average muscle fiber cross-sectional area [$(6.1 \pm 0.1) \times 10^{-5} \text{ cm}^2$], average fiber length ($\leq 2.5\text{-}3 \text{ mm}$), average fiber volume ($1.8 \times 10^{-5} \text{ cm}^3$, overestimated value to avoid overestimate of the efficiency), myosin head concentration within the fiber ($200 \mu\text{mol/l}$, higher than the widely used value of $150 \mu\text{mol/l}$ also to avoid overestimate of the efficiency), the amount of M-ADP-Pi myosin heads immediately before flash activation ($200 \times 10^{-6} \times 1.8 \times 10^{-5} \times 10^{-3} = 3.6 \times 10^{-12} \text{ mol}$). In **Figure 22**, the value of E is maximum at $0.53P_0$ and the corresponding value of P_s is $0.13 P_0$, where P_0 represents the initial amount of M-ADP-Pi myosin heads ($3.6 \times 10^{-12} \text{ mol}$). The number of ATP molecules utilized for work production is calculated to be 2.8×10^{11} ($3.6 \times 10^{12} \times 0.13 \times$

6×10^{23}). Assuming the energy released by ATP hydrolysis to be 50 kJ/mol [16], the energy available from one ATP molecule is $8.3 \times 10^{-20} \text{ J}$ [$(50 \times 10^3)/(6 \times 10^{23})$]. The energy released from ATP molecules for work production is $2.3 \times 10^{-8} \text{ J}$ ($2.8 \times 10^{11} \times 8.3 \times 10^{-20}$). In **Figure 22**, the maximum amount of work done at $0.53 P_0$ is $1.6 \times 10^{-8} \text{ J}$. Thus, the maximum efficiency of individual myosin heads is calculated to be 0.7 [$(1.6 \times 10^{-8})/(2.3 \times 10^{-8})$]. As the above estimation is conservative, the actual efficiency of individual myosin heads is suggested to be $0.8\text{-}0.9$, being close to unity. In this connection, it is of interest that the efficiency of ATP-dependent rotary motion of Fo-F1 ATPase located at the mitochondrial membrane is estimated to be close to unity [22].

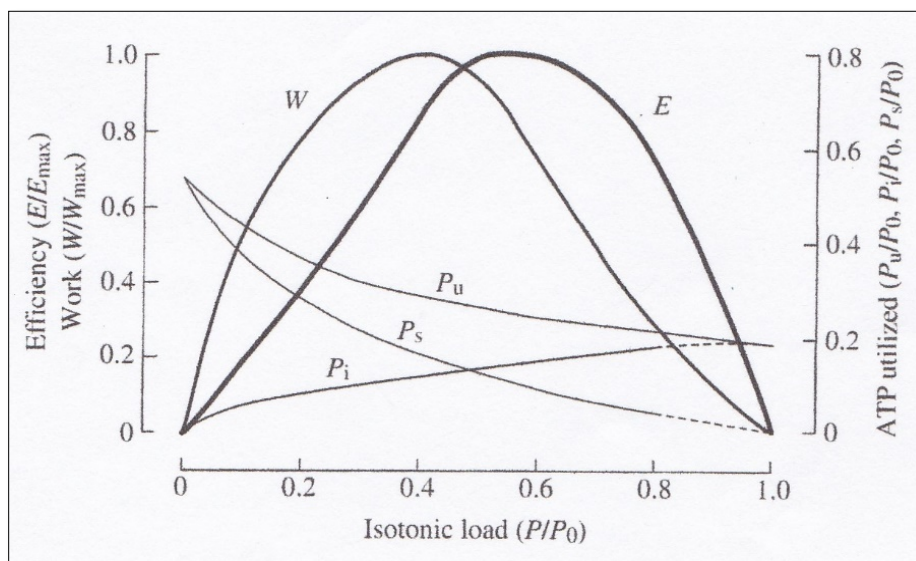


Figure 22. Dependence of the efficiency E of a permeabilized muscle fiber, in which almost all myosin heads are in the state of M-ADP-Pi at the moment of flash activation, on the amount of isotonic load, expressed relative to P_0 . The amount of work done. ATP utilized for the whole mechanical response P_u , for isometric force development preceding shortening P_i , for isotonic shortening P_s , are also shown as functions of load [21].

CONCLUSION

The Fenn effect showed that a muscle can regulate its energy output by somehow sensing the experimental conditions. Although Fenn's experiment was admittedly crude due to a number of uncertainties, especially non uniform sarcomere lengths of component muscle fibers, the Fenn effect can be observed at the levels of permeabilized single muscle fibers, single myofibrils, and in vitro assay systems, in which uncertainties arising from whole muscle are completely removed. Our experimental work described in the last chapter of this review article has indicated that it is the fundamental property of individual myosin heads that regulates energy output by sensing experimental conditions, and this may constitute the main reason that the Fenn effect is always observed at the levels of whole muscles, permeabilized muscle fibers, and even in vitro motility assay systems. Although the Fenn effect can be explained to some extent by the Huxley contraction model, its underlying mechanism as to how individual myosin heads sense experimental conditions to regulate their rate of ATP utilization still remains to be a mystery to be investigated in future. In our opinion, there is a possibility that individual myosin heads may sense the amount of load at the junction between myosin head lever arm domain (LD) and myosin subfragment-2 (S-2), connecting myosin heads to myosin filament backbone, as evidenced by the effect of anti-S-2 and anti-LD antibodies on the strength of actin-myosin binding at the myosin head-actin interface [23,24]. Much more experimental work is necessary to reach full understanding of the mechanism underlying the Fenn effect.

ACKNOWLEDGEMENT

We wish to thank Drs. Iwamoto H, Kobayashi T, Oiwa K and Chaen S for their contribution to the experiments described in this review.

REFERENCES

1. Fenn WO (1923) A quantitative comparison between the energy liberated and the work performed by the isolated Sartorius of the frog. *J Physiol* 58: 175-203.
2. Carlson FR, Wilkie DR (1974) *Muscle Physiology*. Prentice-Hall, New Jersey.
3. Carlson FR, Hardy DJ, Wilkie DR (1963) Total energy production and phosphocreatine hydrolysis in the isotonic twitch. *J Gen Physiol* 46: 851-891.
4. Carlson FR, Hardy DJ, Wilkie DR (1967) The relation between heat produced and phosphocreatine split during isometric contraction of frog's muscle. *J Physiol* 189: 209-235.
5. Marechal G, Monnmaerts WFHM (1963) The metabolism of phosphocreatine during an isometric tetanus of frog Sartorius muscle. *Biochem Biophys Acta* 70: 53-67.
6. Sandberg JA, Carlson FR (1966) The length dependence of phosphocreatine hydrolysis during an isometric tetanus. *Biochem Z* 345: 212-231.
7. Cain DF, Davies RE (1962) Breakdown of adenosine triphosphate during a single contraction of working muscle. *Biochem Biophys Res Commun* 8: 361-366.
8. Cain DF, Infante AA, Davies RE (1962) Chemistry of muscle contraction *Nature* 196: 214-217.
9. Infante AA, Davies RE (1965) The effect of 2,4-dinitrofluorobenzene on the activity of striated muscle. *J Biol Chem* 240: 3996-4001.
10. Kushmerick MJ, Davies RE (1969) The chemical energetics of muscle contraction II. The chemical efficiency and power of maximally working Sartorius muscle. *Proc R Soc B* 175: 315-343.
11. Woledge RC, Curtin NA, Homsher E (1985) *Energetic aspects of muscle contraction*. Academic Press, London.
12. Sugi H (1992) *Muscle contraction and cell motility: molecular and cellular aspects*. Adv Comp Environ Physiol Springer, Heidelberg.
13. Ebashi S, Endo M (1968) Calcium ion and muscle contraction. *Prog Biophys Mol Biol* 18: 125-183.
14. Chaen S, Shimada M, Sugi H (1986) Evidence for cooperative interaction of myosin heads with thin filament in the force generation of vertebrate skeletal muscle fibers. *J Biol Chem* 261: 13632-13636.
15. Potma EJ, Stienen GJ (1996) Increase in ATP consumption during shortening in skinned fibres from rabbit psoas muscle: Effects of inorganic phosphate. *J Physiol* 496: 1-12.
16. He ZH, Chillingsworth RK, Brune M, Corrie JET, Trentham DR, et al. (1999) ATPase kinetics on activation of rabbit and frog permeabilized isometric muscle fibres: A real time phosphate assay. *J Physiol* 501: 125-148.
17. Chaen S, Shirakawa I, Bagshaw CR, Sugi H (1997) Measurement of nucleotide release kinetics in single skeletal muscle myofibrils during isometric and isovelocity contractions using fluorescence microscopy. *Biophys J* 73: 2033-2042.
18. Oiwa K, Chaen S, Sugi H (1991) Measurement of work done by ATP-induced sliding between rabbit muscle myosin and algal cell actin cables *in vitro*. *J Physiol* 437: 751-763.
19. Huxley AF (1957) *Muscle structure and theories of contraction*. *Prog. Biophys Biophys Chem* 7: 255-318.
20. Sugi H, Iwamoto H, Akimoto T, Ushitani H (1998) Evidence for the load-dependent mechanical efficiency of individual myosin heads in skeletal muscle fibers

activated by laser flash photolysis of caged calcium in the presence of a limited amount of ATP. Proc Natl Acad Sci U S A 95: 2273-2278.

21. Sugi H, Iwamoto H, Akimoto T, Kishi H (2003) High mechanical efficiency of the cross-bridge power stroke in skeletal muscle. J Exp Biol 206: 1201-1206.
22. Kinoshita Jr, Yasuda R, Noji H, Adachi K (2000) A rotary molecular motor that can work at near 100% efficiency. Phil Trans R Soc B 355: 473-489.
23. Sugi H, Kobayashi T, Gross T, Noguchi K, Karr T, Harrington WF (1992) Contraction characteristics and ATPase activity of single muscle fibers in the presence of antibody to myosin subfragment-2. Proc Natl Acad Sci U S A 89: 6134-6137.
24. Sugi H, Chaen S, Kobayashi T, Abe T, Kimura K, Saeki Y, et al. (2014) Definite differences between in vitro actin-myosin sliding and muscle contraction as revealed using antibodies to myosin head. PLoS One 9: e93272.